Meteorological drivers of hypolimnetic anoxia in a eutrophic, north temperate lake

Craig A. Snortheim [a,*], Paul C. Hanson [a], Katherine D. McMahon [a], Jordan S. Read [b], Cayelan C. Carey [c], Hilary A. Dugan [a]

[a] Center for Limnology, University of Wisconsin – Madison, Madison, WI, USA
[b] Center for Integrated Data Analytics, U.S. Geological Survey, Middleton, WI, USA
[c] Department of Biological Sciences, Virginia Tech, 1405 Perry Street, Blacksburg, VA, USA

ARTICLE INFO

ABSTRACT

Oxygen concentration is both an indicator and driver of water quality in lakes. Decreases in oxygen concentration leads to altered ecosystem function as well as harmful consequences for aquatic biota, such as fishes. The responses of oxygen dynamics in lakes to climate-related drivers, such as temperature and wind speed, are well documented for lake surface waters. However, much less is known about how the oxic environment of bottom waters, especially the timing and magnitude of anoxia in eutrophic lakes, responds to changes in climate drivers. Understanding how important ecosystem states, such as hypolimnetic anoxia, may respond to differing climate scenarios requires a model that couples physical-biological conditions and sufficiently captures the density stratification that leads to strong oxygen gradients. Here, we analyzed the effects of changes in three important meteorological drivers (air temperature, wind speed, and relative humidity) on hypolimnetic anoxia in a eutrophic, north temperate lake using the anoxic factor as an index that captures both the temporal and spatial extent of anoxia. Air temperature and relative humidity were found to have a positive correlation with anoxic factor, while wind speed had a negative correlation. Air temperature was found to have the greatest potential impact of the three drivers on the anoxic factor, followed by wind speed and then relative humidity. Across the scenarios of climate variability, variation in the simulated anoxic factor was primarily due to changes in the timing of onset and decay of stratification. Given the potential for future changes in climate, especially increases in air temperature, this study provides important insight into how these changes will alter lake water quality.

© 2016 Elsevier B.V. All rights reserved.

1. Introduction

Lake eutrophication has led to degradation of water quality in lakes and reservoirs at a global scale (Diaz 2001; Carpenter et al., 2011; Trolle et al., 2011; Kara et al., 2012). An important consequence of elevated productivity in eutrophic systems is anoxia (<1 mg O_2 L^{-1}) in lake bottom waters (the hypolimnion), which arises from increased microbial metabolism of degradable organic matter (OM) (Hanson et al., 2004; Cooke et al., 2005; Bouffard et al., 2013). In thermally stratified lakes, in which the hypolimnetic waters are effectively isolated from atmospheric and photosynthetic oxygen sources in the epilimnetic surface waters,

hypolimnetic dissolved oxygen (DO) consumption by microbial respiration leads to oxygen depletion and eventually anoxia (Robertson and Imberger 1994; Nürnberg 1995; Foley et al., 2012). Anoxia is a serious environmental threat, as it leads to the release of nutrients such as phosphorus (P) and metals from the sediments into the water column, and has negative consequences for fish and macroinvertebrates, including altered spatial distribution of species, changes in physiological processes and predator-prey interactions, and potentially death (Arend et al., 2011; Foley et al., 2012).

Projected changes in meteorological drivers over the next century are likely to cause further deterioration of water quality globally and may undermine management strategies intended to decrease anoxia (Jeppesen et al., 2007, 2009; Williamson et al., 2009; Trolle et al., 2011). Changes in water temperature and oxygen dynamics are occurring in many lakes worldwide (e.g. Hampton

* Corresponding author.
   E-mail address: csnortheim@gmail.com (C.A. Snortheim).

et al., 2008; Williamson et al., 2009; Schneider and Hook 2010; Foley et al., 2012; Palmer et al., 2014; North et al., 2014). However, the links between meteorological drivers and lake responses are complex. In some studies, there is evidence of diurnally asymmetric effects (i.e., a differing effect in the magnitude between daytime and nighttime) of meteorological drivers such as air temperature or wind speed (Livingstone 2003; Wilhelm et al., 2006; Kerimoglu and Rinke, 2013). Other studies, using model forecasts, have predicted increased stratification strength and duration, which would likely lead to increased extent of anoxia in the future (Mackay et al., 2009; Samal et al., 2012). Consequently, it is important to understand how changes in multiple meteorological drivers interact to affect important seasonal oxygen dynamics.

In linking meteorological drivers to water quality in lake ecosystems, most work has focused on the relationships between air temperature, longwave radiation, and lake thermal structure (Trolle et al., 2011; Samal et al., 2012), and there is still a need for investigating the effects and interactions of other meteorological drivers, such as wind speed, on thermal structure, as well as the subsequent chemical and biological responses to altered thermal structure (Wilhelm et al., 2006; Mackay et al., 2009; Kerimoglu and Rinke, 2013). For example, increased wind speeds cause increased surface turbulence, acting to decrease thermal stability. This can lead to delayed stratification and induce earlier fall turnover, potentially shortening anoxia duration. The complex interactions between exogenous forcings and lake anoxia are challenging to understand and require an analytical framework that both couples physics and biology within lakes and accounts for vertical thermal and chemical gradients.

Process-based numerical simulation models are appropriate for studies of meteorological scenarios because lakes have complex physical-biological coupling and substantial temporal variance (Arhonditsis et al., 2006; Kara et al., 2012). A number of factors may determine the spatial extent and duration of hypolimnetic anoxia, including epilimnetic productivity, duration of thermal stratification, thermal stability, hypolimnetic temperature, and hypolimnetic volume (Foley et al., 2012; Müller et al., 2012; Bouffard et al., 2013). Additionally, these processes are not independent of each other and may affect hypolimnetic anoxia in contrasting ways. As an example, higher hypolimnetic water temperatures can favor increased microbial metabolism rates and thus increased anoxia duration (i.e. earlier anoxia onset) (Foley et al., 2012), but they can also lead to decreased thermal stability, thereby decreasing the spatial extent and duration of anoxia (Nürnberg, 1988). Further, many heat-flux processes controlling thermal structure, and thus influencing chemical and biological processes throughout the water column, are non-linear (Wilhelm et al., 2006). Process-based numerical models are able to simulate these complex interactions and feedbacks between physics and biogeochemistry (Hamilton and Schladow, 1997), and thus are well-suited to provide insight into how oxygen dynamics may change under a gradient of meteorological scenarios.

How do meteorological drivers affect hypolimnetic oxygen dynamics in a eutrophic, north temperate lake? Does the timing of perturbations in meteorological drivers (day vs. night) influence their effect on oxygen dynamics? What are the projected impacts of changing climate on lake oxygen dynamics for the latter half of the 21st century? To explore these questions, we used a process-based, one-dimensional, hydrodynamic-biogeochemical lake model calibrated to observational data to independently test the influence of meteorological variables on lake anoxia, as well as explore meteorological scenarios that may be outside the bounds of available observational data. We applied this model to a well-studied eutrophic, north temperate lake (Lake Mendota, Wisconsin, USA) that routinely experiences hypolimnetic oxygen depletion during summer stratification. We examined relationships between

changes in meteorological driving variables and emergent properties of the lake system using simple statistical models.

2. Methods

2.1. Study site description

Lake Mendota is a dimictic, eutrophic lake located in south-central Wisconsin, USA (43°7′N, 89°25′W). It has a surface area of 39.4 km^2 and a maximum depth of 25.3 m (Brock, 1985; Kitchell, 1992). Lake Mendota's major tributary, the Yahara River, accounts for approximately 70% of the total annual inflow. The hydraulic residence time is roughly 6 years. The lake is typically frozen from late December until early April, and stratifies June through early October. Due to its eutrophic status since the mid-1800s, Lake Mendota experiences intense phytoplankton blooms and hypolimnetic anoxia each summer (Brock, 1985).

2.2. Anoxic factor calculation

Anoxia is the state of extremely low DO, which can occur in the hypolimnion of a lake during thermal stratification when the bottom waters are isolated from atmospheric and photosynthetic oxygen sources in the surface waters. During this period, DO consumptive processes, or sinks, such as microbial respiration, exceed DO sources (downward transport from the surface waters via advection and diffusion), and DO decreases to very low concentrations. In this study, the anoxic threshold is defined as 1 mg L^{-1} (Nürnberg, 1995; Foley et al., 2012). The *anoxic factor (AF)* is an index that summarizes both the temporal duration and spatial extent of anoxia in a lake or reservoir into a single value for a specified length of time (e.g., a summer season) (Nürnberg, 1995). Anoxic factor (Nürnberg, 1995; Marcé et al., 2010) or other similar indices such as 'hypolimnetic anoxia' (Foley et al., 2012) and 'hypoxic factor' (North et al., 2014) have been used to track changes in hypolimnetic oxygen concentrations across varying meteorological conditions. The AF represents the amount of time (t) that a sediment area (a), normalized by the surface area of the lake (A_0), is overlain by anoxic waters (Eq. (1)).

$$AF = \frac{\sum_{i=1}^{n} t_i a_i}{A_o} \tag{1}$$

AF captures the spatial extent of anoxia by considering the anoxic depth in the water column (Fig. 1) and is normalized by lake surface area, allowing for comparison among lakes. AF is reported in time units (days), but is often described as days year^{-1} or days season^{-1} to specify whether winter anoxia (under ice) is included or excluded, respectively, in the AF calculation (Nürnberg, 1995). Because AF accounts for both the duration and spatial extent of anoxia, it is more indicative of the physiochemical and ecological impact of anoxia on a lake system than anoxia duration or the oxygen depletion rate. For example, if the time of stratification formation and decay were identical for two separate years for an idealized lake, but the oxycline depth differed, the measures of anoxia duration for the two years would be the same but the anoxic factor measures would differ.

2.3. Simulation model

We used a hydrodynamic-biogeochemical model to explore how changes in external forcing alter AF. While AF can be calculated directly from observational data, the model enabled us to explore gradients not represented in the observational data, the sensitivities of AF to relatively small changes in meteorology that may be masked by noise in the observational data, and to simulate the
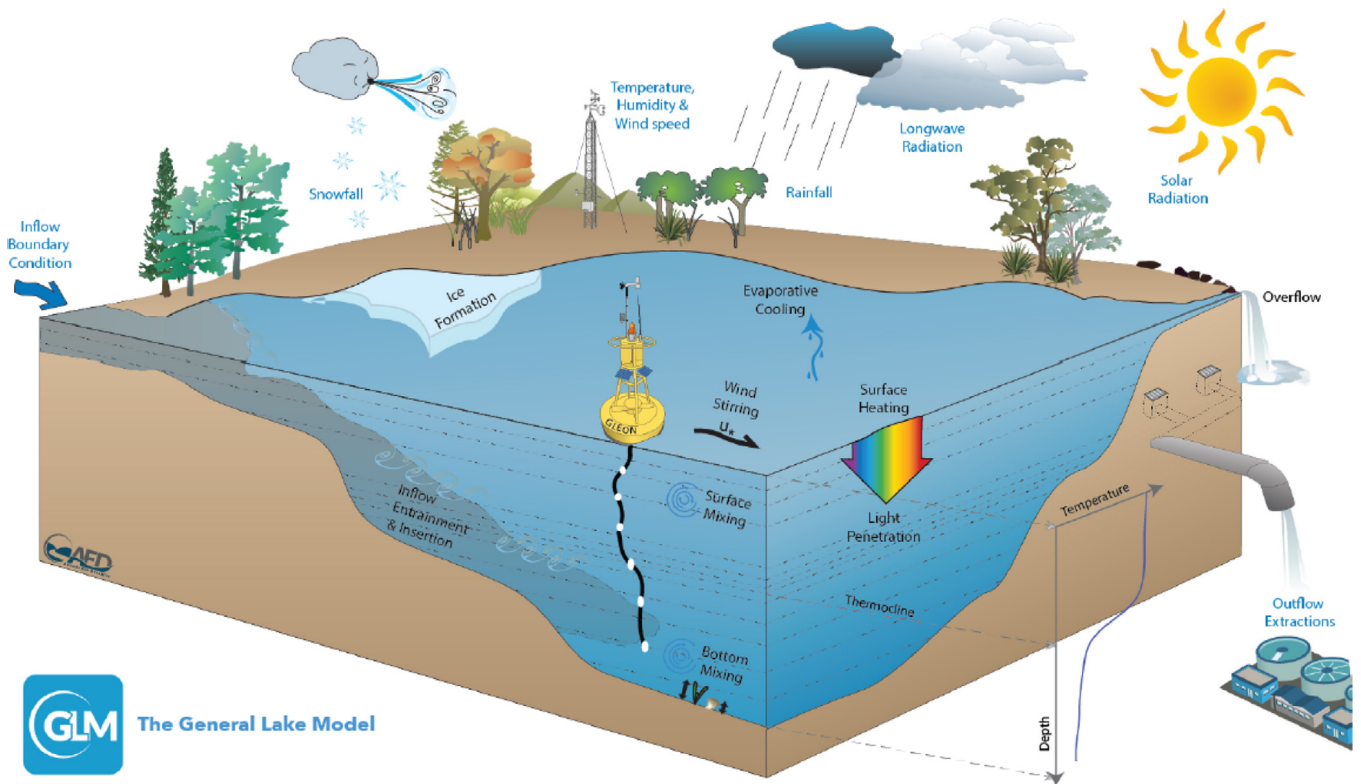
Fig. 1. Conceptual model of the General Lake Model (adapted from Hipsey et al., 2014), illustrating the effects of exogenous drivers on lake physical processes.
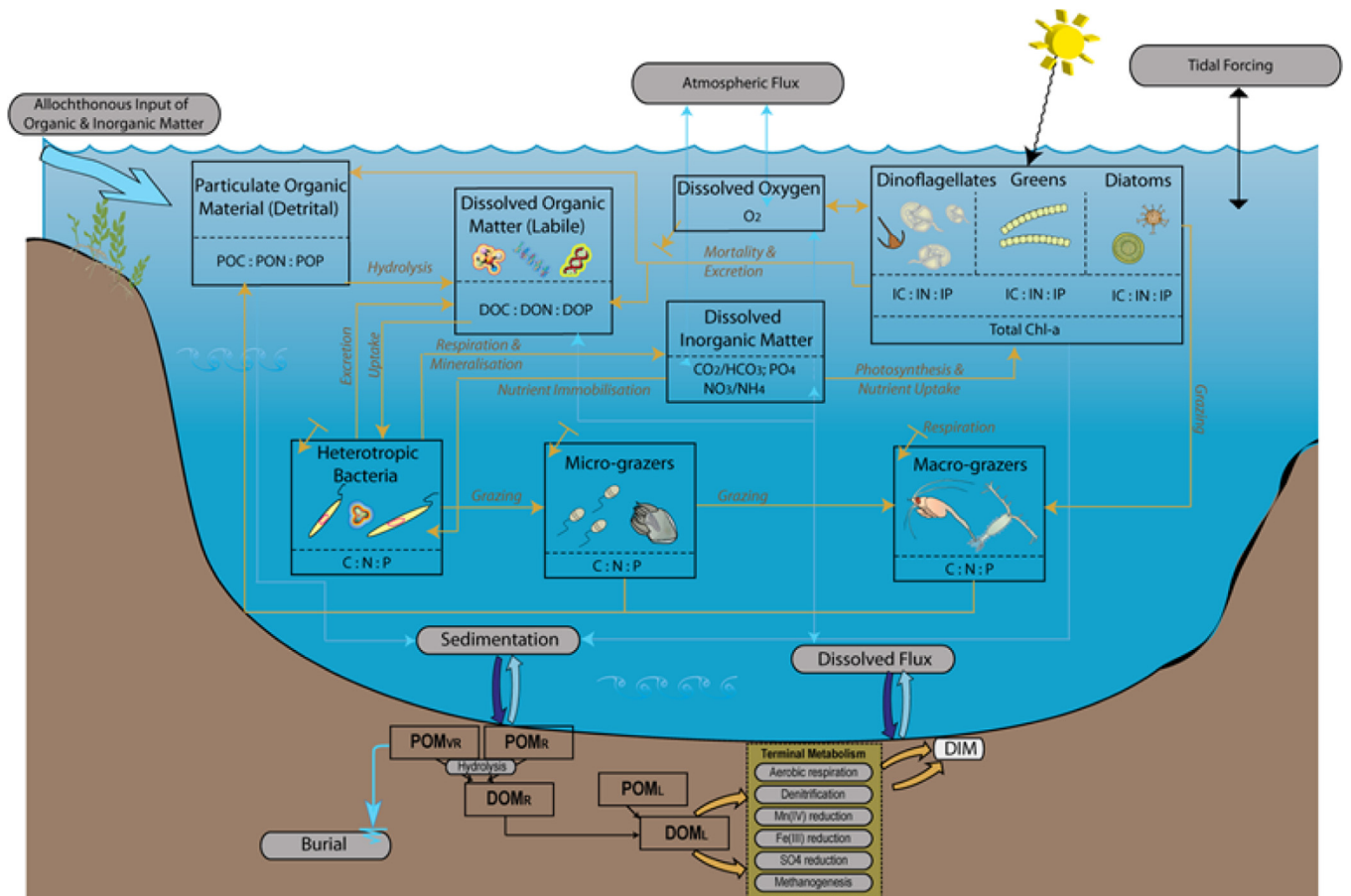

Fig. 2. Conceptual model of the Aquatic EcoDynamics modules (adapted from Hipsey et al., 2013), illustrating key chemical and biological processes. The bacteria and zooplankton modules were not included in this study.

independent effects of meteorological drivers that are correlated in the observational data. Moreover, the simulation framework allowed us to generate many meteorological scenarios not available in the observational data. We used the General Lake Model (GLM v1.4.0), a one-dimensional (1D) vertical stratification model coupled through the Framework for Aquatic Biogeochemical Modeling (FABM) to the Aquatic EcoDynamics module library (AED) (Hipsey et al., 2013, 2014) (Figs. 1 and 2 Fig. 2). The model uses a flexible Lagrangian layer structure which allows the number and thickness of vertical layers to vary through time (subject to user-defined constraints of 0.1 to 1 m thickness for our simulations) in order to sufficiently resolve the vertical gradients. Layers can expand, contract, merge or split in order to simulate water balance, mixing and stratification. Physical, chemical and biological variables are assumed constant within each layer. The reader is referred to the science manuals for GLM (http://aed.see.uwa.edu.au/research/models/GLM/overview.html) and AED (http://aed.see.uwa.edu.au/research/models/AED/Pages/documentation.html) for further information regarding the model process equations, state variables and parameters.

The GLM-FABM-AED model (referred to as 'GLM-AED' hereafter) was well-suited for this study because of its: (1) open source availability and transparency, which encourages future repeatability of these experiments; (2) flexibility, through AED's modular design, in the types of ecological processes included in the simulation; (3) low computational requirements for a single run, thus enabling repeated experiments that include thousands of simulations. Further, many of the heat transfer and mixing algorithms have been adopted from Hamilton and Schladow (1997) and have been tested extensively through a wide range of conditions in the DYnamic REervoir Simulation Model (DYRESM) (Gal et al., 2009; Trolle et al., 2008, 2011; Bruce et al., 2006). In calculating AF from 1D model results, we implicitly assume spatial homogeneity (except for the vertical dimension). This has previously been shown to be a valid assumption for chemical state variables within the hypolimnion of Lake Mendota (Kamarainen et al., 2009).

2.4. Model setup & observational data

The model was initialized and calibrated using driver data and water quality data from 2009 and 2010. Validation was conducted using data from 2007 and 2008. This time period was chosen as it represented the highest-quality data available at the inception of this study. Years 2009 and 2010 were used as the calibration years because they represented the years of the lowest and highest observed anoxic factor, respectively, allowing calibration to cover the widest possible range of anoxic conditions. High-frequency (min^{-1}, down-sampled to $hour^{-1}$ for this study) water temperature data were available from an instrumented buoy located near the geographic center of Lake Mendota (http://metobs.ssec.wisc.edu/buoy). All water quality data were collected and analyzed according to standardized protocols through the North Temperate Long-Term Ecological Research program, which also samples at the buoy site (https://lter.limnology.wisc.edu/). Water quality data were generally available at a biweekly temporal interval and at 4-m spatial (depth) interval, with chemical data (dissolved oxygen, nitrate, phosphate, etc.) available throughout the water column and phytoplankton data typically available at 0–8 m depth from the surface. Meteorological data were collated from multiple sources (Table 1).

Simulations were run for individual open water seasons (approximately mid-April through December) to focus on anoxia that occurs in the summer stratified period. The simulation time step was one hour, aligning with the hourly meteorological driver data. The results output time step was set to 12 h to capture diurnal dynamics but also to minimize model output file sizes. Therefore, the model output had a temporal resolution of 12-h and a spatial

(depth) resolution reflecting the number of model layers at that simulation time step (maximum layer thickness of 1 m). To calculate goodness-of-fit metrics, each available observed data point was matched in time and space (depth) to the modeled results, using linear interpolation on the modeled data when required.

AED modules representing ecosystem processes that were expected to have particular relevance to anoxia were included. We simulated oxygen, nutrients (silica, nitrogen, and phosphorus), organic matter, and phytoplankton. These processes are especially important in eutrophic Lake Mendota, where phytoplankton account for the major organic carbon flux that fuels microbial respiration in deeper waters (Brock, 1985). Within the phytoplankton module, four functional groups were simulated to account for most of the planktonic organic carbon biomass: *Microcystis* (non-N-fixing cyanobacteria in *Microcystis* genus), *Aphanizomenon* (N-fixing cyanobacteria in the *Aphanizomenon* or *Anabaena* genera), chlorophytes (all remaining green algae), and diatoms (all phytoplankton in the Bacillariophyta division) (Kara et al., 2012). Phytoplankton mortality was subsumed into the phytoplankton respiration parameters, allowing for regulation without enabling a zooplankton functional group (Hipsey et al., 2013). Heterotrophic bacterial respiration processes were captured through sediment oxygen demand and water column respiration via the mineralization of dissolved organic carbon (DOC).

2.5. Model calibration

Both automated and manual calibration routines were conducted to optimize the goodness-of-fit for the subsequently mentioned state variables that are known to influence hypolimnetic anoxia. We calibrated water level and water temperature (WT) to ensure the model was sufficiently representing lake level and stratification. We also calibrated DO and nutrients, including filterable reactive phosphorus, nitrate, ammonium, dissolved reactive silica, DOC, dissolved inorganic carbon (DIC), as well as the biomass of each of the four phytoplankton functional groups to ensure adequate representation of the contribution of phytoplankton to the OC pool that subsidizes heterotrophic respiration. Because a GLM-AED model with multiple phytoplankton functional groups has hundreds of total parameters, we focused our calibration efforts on the most influential parameters directly related to each of the target state variables. Sensitivity of predictions to changes in model parameters was ranked by the variation of the fit metric (Root Mean Square Error (RMSE) or Normalize Mean Absolute Error (NMAE)) in response to approximately ± 30% changes in the default parameter values (Bruce et al., 2006; Gal et al., 2009; Kara et al., 2012). All calibrated parameters and final assigned values can be found the Appendix tables (Tables A1–A3).

Calibration of physical and chemical state variables involved minimizing NMAE via adjustments to the target parameters within literature ranges. The minimization routine was executed by constrained, nonlinear, multidimensional optimization in R, tuning up to five parameters simultaneously (Nelder and Mead 1965; R Development Core Team, 2014). The R language was chosen because it is open source, flexible, and platform independent. For phytoplankton functional groups, calibration was accomplished via manual, incremental adjustments to the top five most sensitive phytoplankton parameters (Table A3) to find the best qualitative match to observed data. Emphasis was placed on seasonal mean and peak timing and magnitude, as these characteristics are important features of phytoplankton dynamics (Rigosi et al., 2011). The final applied parameter values were the mean of the results of the two independent manual calibration routines for the 2009 and 2010 seasons.

The model was calibrated to best match the observed time series data at all depths for the state variables, with equal weight-

Table 1
Sources of data for meteorological driver variables. Longwave radiation values were calculated following procedures from Crawford and Duchon (1999).

Meteorological Variables	Time Range	Data Source	Website
Air temperature, wind speed, relative humidity, shortwave radiation	2007–2010	University of Wisconsin Space Science and Engineering Ground-Based Atmospheric Monitoring Suite (UW-SSEC/AOS)	http://metobs.ssec.wisc.edu/aoss/tower/
Rain, snow; supplemental air temperature, wind speed, relative humidity	2007–2010	National Climatic Data Center (NCDC)	http://www.ncdc.noaa.gov/
Supplemental shortwave radiation	2007–2010	National Oceanic and Atmospheric Administration's (NOAA) Earth System Research Laboratory Global Monitoring Division (ESRL-GMD)	http://www.esrl.noaa.gov/gmd/
All variables, for observed data MLR model	1995–2011	North American Land Data Assimilation System (NLDAS)	http://ldas.gsfc.nasa.gov/nldas/

ing placed on each depth (i.e. no volumetric weighting). GLM-AED model was not calibrated for AF because it could force a numerical agreement of the indices while obscuring the spatial-temporal dynamics of some state variables in a way unrepresentative of the system.

2.6. Climate scenarios

We focused our study on air temperature, wind speed and relative humidity (RH), three meteorological driver variables that are critical components of the lake's surface energy budget, and held the water balance constant (i.e. precipitation and streamflow). Scenarios involved the simultaneous application of constant, additive changes to the observed hourly time series of these meteorological variables for a single open-water season in the 2007–2010 simulation period (i.e. four different baseline years). Along with all-day perturbation scenarios (i.e. change applied to all hourly time points), scenarios were executed for daytime perturbations only and for nighttime perturbations only. A single scenario run included four steps in which scenario information flowed from the original meteorological ("met") file in the form of perturbations, through the GLM-AED simulation and post-processing, and ultimately to the AF value (Fig. 3).

In step 1, perturbations for air temperature, wind speed and RH were randomly sampled from a uniform distribution of perturbation ranges that were based on the magnitude of projected changes in the three meteorological variables. The projected changes were derived from the GENMOM GCM with A2 emission scenario downscaled to Lake Mendota following the methods of Hostetler et al., 2011. The range of perturbations was centered at zero, and set to encompass the maximum projected change in the monthly mean values between the periods 2070–2089 and back-projected 1980–1999 (in order to capture longest available time period and thus likely the largest projected change). The resulting perturbation ranges were $\pm 3\,°C$ for air temperature, $\pm 0.25\,m\,s^{-1}$ for wind speed, and $\pm 6\%$ for relative humidity. The constant, additive perturbations were applied to all applicable hourly time steps (all-day, daytime or nighttime), representing a shift in the mean value of the meteorological driver variable. For example, daytime perturbations scenarios involved changes only to hourly time points during the day, while nighttime driver data remained identical to the baseline. Day and night were distinguished by a $10\,W\,m^{-2}$ threshold of shortwave radiation values, and over the simulation periods, there was an even split between day and night hourly time points ($50\% \pm 0.4\%$ for all baseline years). Longwave radiation was not a target climate driver in this study, but was adjusted to reflect changes in air temperature and relative humidity following Crawford and Duchon (1999). This allowed for all climate scenarios to be as realistic as possible while allowing for independent perturbations in air temperature, wind speed, and relative humidity.

In step 2, a GLM-AED simulation was executed using the adjusted (scenario) meteorological driver data (Fig. 3). DO data were read from the simulation results in step 3. In step 4, the AF was calculated and recorded. This value, along with scenario information such as the perturbation timing and the perturbation magnitudes, was recorded and then the process was repeated by launching another scenario from step 1. This process was repeated 500 times for each of three perturbation timings (all-day, daytime, and nighttime) and for each of four baseline years (2007–2010). This resulted in a total of $500 \times 3 \times 4 = 6000$ simulations. The R package 'glmtools', in conjunction with additional customized R code, was used to set up and execute simulations as well as extract, format, statistically analyze, and visualize data from the NetCDF output files (Read et al., 2014).

2.7. Statistical analyses of simulation & observational data

We conducted multiple linear regression (MLR) analysis using the change in AF from baseline as a response variable and the shift in each of the three meteorological variables as independent variables (Eq. (2)).

$$\Delta AF = C_{AT}\left(\Delta AT\right) + C_{WS}\left(\Delta WS\right) + C_{RH}\left(\Delta RH\right) \tag{2}$$

This allowed us to determine if shifts in the mean air temperature, wind speed and relative humidity for an open-water season could be used to predict how much the AF shifted from the long-term mean. While a complex simulation model is needed to predict the onset and conclusion of hypolimnetic anoxia, as well as the spatial extent at any given time, we were interested in testing whether a simple statistical model could adequately capture an emergent property of the lake system through a season (i.e. the AF). We assessed the 'adequacy' of the statistical models by analyzing the residual plots to ensure normality, linearity, homoscedasticity, and absence of outliers (Foley et al., 2012). We tested for correlation amongst the predictor variables for both simulation and observational data using the Pearson correlation coefficient. Longwave radiation was not included in the regression analysis to avoid multicollinearity.

The sign of each of the three meteorological variable coefficients reveals the direction of the influence of each of the meteorological drivers (i.e. tendency to increase or decrease AF), and the coefficient magnitudes provide effect estimates. Statistical comparison of the coefficients derived from daytime-perturbation simulations and nighttime-perturbation simulations revealed whether or not there existed significant differences between daytime and nighttime effects. Finally, since AF incorporates both the spatial and temporal extent of anoxia, we used simple regression to test how a spatial (thermocline depth) and temporal (anoxia duration) emergent property of the lake system accounted for the variability in the simulated AF.

To check our findings derived from simulation data against observed data, we conducted MLR analysis using observed mete-
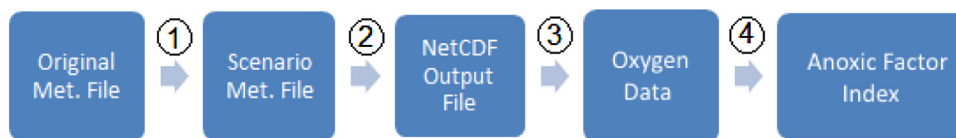
Fig. 3. Workflow diagram depicting the processing steps for a model run from baseline simulation files to derived summary indices from scenario results. (1) Perturbations for air temperature, wind speed and relative humidity were applied to the original meteorological data file. (2) The GLM-AED model was run with scenario meteorological driver data. (3) Simulated oxygen data were extracted from the NetCDF output file. (4) Simulated data were processed to derive the simulated anoxic factor.

orological and DO data for the period 1995–2011 (n = 17). Meteorological data used in this analysis were hourly observations from NLDAS, and DO data were biweekly to monthly profile measurements from NTL-LTER. We calculated perturbations using the long-term mean value during the open water season as a baseline. Although there is relatively low statistical power with just 17 observation years available (compared to thousands of scenario simulations), we performed this analysis of the observational data to test whether or not the simulation results agreed with historically observed meteorological conditions and the corresponding observed AF value.

2.8. Extremes testing

We evaluated the simulated AF response across a wide state space of meteorological variable conditions, including some outside the bounds of observed data, in order to gain a better understanding of how extreme a change must be to force a particular system response. Scenarios were run with air temperature perturbations of $\pm 15\,^{\circ}$C, wind speed perturbations of $\pm 2\,\mathrm{m\,s^{-1}}$, and relative humidity perturbations of ± 15 percent, with longwave radiation adjusted accordingly. The year 2009 was selected as a baseline because this year offered high-quality data that was represented a near-average open water season for Lake Mendota in terms of key state variables such as water temperature. Perturbations were applied for all-day exposures and response surfaces were developed for each of the three two-way interactions (Kerimoglu and Rinke, 2013).

3. Results

3.1. Calibration results

The GLM-AED model was able to reproduce the observed physical, chemical, and biological variables of interest in Lake Mendota (Table 2, Fig. 4) (see Methods section for details on observed/modeled data resolution and NMAE calculation). NMAE values for physical and chemical state variables fell within reported literature ranges from studies of numeric simulation of lakes, except for epilimnetic DO and both epilimnetic and hypolimnetic DOC and DIC (Table 2). Despite being slightly outside literature ranges, the results of this study were found to be insensitive to epilimnetic DO, and the DOC/DIC NMAE values were within normal ranges for chemical state variables. Simulated total phytoplankton dynamics showed relatively good agreement with observed data; however, the simulation was unable to reproduce a large *Aphanizomenon* bloom observed in 2008 (Fig. 5). Finally, AF values derived from simulated data showed agreement with those derived from observed data (Fig. 6).

3.2. MLR analysis of simulation results

Statistical models of the simulation results showed that the three meteorological drivers were highly significant predictors of the simulated AF (all $p \leq 0.001$). All-day increases in air temperature and relative humidity increased the simulated AF by 4.24 days $^{\circ}$C^{-1}

and 0.464 days RH%$^{-1}$ respectively, while changes in wind speed altered the simulated AF by -15.9 days $(\mathrm{m\,s^{-1}})^{-1}$. The effects of changing meteorological drivers during only daytime or nighttime were less than the all-day effects (Table 3, Fig. 7a–c), suggesting a positive correlation with exposure time. However, the effect was not always proportional to the time of exposure. For example, the effect of nighttime wind speed perturbations was -14.0 days $(\mathrm{m\,s^{-1}})^{-1}$, or 88% of the all-day effect (Table 3). When the effects of daytime vs. nighttime wind speed perturbations on AF were compared directly, without accounting for random perturbations in air temperature or RH in the statistical model, the nighttime wind speed perturbation effect $(-11.6$ days $(\mathrm{m\,s^{-1}})^{-1})$ was statistically greater $(p < 0.001)$ than the daytime wind speed perturbation effect $(-7.57$ days $(\mathrm{m\,s^{-1}})^{-1})$ (Fig. 7e). When similarly compared, the daytime air temperature perturbation effect $(2.19$ days $^{\circ}$C$^{-1})$ was statistically greater $(p < 0.001)$ than the nighttime perturbation effect of air temperature on AF $(1.92$ days $^{\circ}$C$^{-1})$ (Fig. 7d). There was no statistical difference between daytime and nighttime RH effects $(p > 0.1)$ (Fig. 7f).

We investigated the contributions of anoxia duration and anoxic area to ΔAF using regression analysis of the simulation results from all-day driver perturbations scenarios. Anoxia duration described 78% of the variability in AF and mean thermocline depth described 21% of the variability in AF. This suggests that within the state space of climate projections, the majority of future changes in AF will likely be a result of changes in the timing of stratification processes. Further, the day of stratification onset and the day of stratification end (defined by a 1 $^{\circ}$C water temperature difference between surface/bottom waters sustained for at least 30 days) accounted for 62 and 54% of the variability in AF, respectively, suggesting approximately equal contributions.

MLR analysis was also conducted for other physical, chemical and biological lake state indices to attempt to better understand the relationships between the meteorological drivers and lake state variables, as well relationships and intersections with anoxia. This analysis is supplementary to our primary analysis of AF, and thus we present only some highlights. There was a strong relationship (all $p \leq 0.001$) between each of the three meteorological drivers and onset of stratification, end of stratification, and the mean thermocline depth. In response to a 3 $^{\circ}$C increase in air temperature, the statistical models predicted stratification onset would occur 6 days earlier, end 2 days later, and the mean thermocline depth would be 1-m less (shallower)- each of which would act to increase AF. A statistically significant (all $p \leq 0.001$) relationship existed between each meteorological drivers and mean hypolimnetic phosphate concentration. However, the statistical model projected just a 0.02 mg-P/L^{-1} increase in mean hypolimnetic phosphate concentration in response to a 3 $^{\circ}$C increase in air temperature. Finally, there was a significant relationship (all $p \leq 0.01$) between air temperature and RH and both mean total phytoplankton and maximum total phytoplankton, but not for wind speed. Increases in air temperature and RH were predicted to decrease both mean and maximum total phytoplankton, albeit by a magnitude of <0.5 mg-C/L^{-1} for our climate scenarios.

Table 2

Model calibration and validation results as normalized mean absolute errors (NMAE) and the coefficient of determination (R^2). Values presented are the mean of the results of the two calibration or validation years. Neither metric incorporated volumetric weighting. Literature range represents numeric simulation studies on several different lakes.

State Variable	Calibration (2009 and 2010)		Validation (2007 and 2008)		Literature Range
	NMAE	R^2	NMAE	R^2	NMAE
Water temperature (WT)	0.062	0.91	0.066	0.79	0.037[d]–0.084[d]
Dissolved oxygen (DO)	0.32	0.53	0.37	0.47	0.054[d]–0.32[a]
Hypolimnetic dissolved oxygen	0.14	0.85	0.18	0.75	0.29[c]
Nitrate (NO_3^-)	0.39	0.87	0.65	0.78	0.28[a]–1.15[d]
Ammonium (NH_4^+)	0.52	0.71	0.43	0.73	0.66[b]–1.8[a]
Filterable reactive phosphorus (PO_4^{3-})	0.36	0.69	0.61	0.73	0.81[b]–1.6[a]
Dissolved reactive silica (DRS)	0.56	0.69	0.48	0.67	–
Dissolved organic carbon (DOC)	0.21	0.50	0.29	0.48	0.053[a]
Dissolved inorganic carbon (DIC)	0.26	0.26	0.34	0.50	0.053[a]

[a] Kara et al. (2012) (values from three month period).
[b] Bruce et al. (2006).
[c] Gal et al. (2009).
[d] Trolle et al. (2011) (uses mean relative absolute error (RE)).

Table 3

Coefficients and standard errors for MLR models that predicted changes in anoxic factor from changes in meteorological drivers ($N_{individual} = 500$, $N_{pooled} = 2000$, $N_{observed} = 17$).

Time of Day	Baseline	Air Temperature Coefficient [days °C^{-1}]	Wind Speed Coefficient [days (m s^{-1})$^{-1}$]	Relative Humidity Coefficient [days%$^{-1}$]
All-day	2007	4.83 ± 0.07	-15.9 ± 0.9	0.491 ± 0.036
	2008	3.96 ± 0.09	-20.1 ± 1.0	0.440 ± 0.043
	2009	3.63 ± 0.08	-12.5 ± 0.9	0.386 ± 0.040
	2010	4.23 ± 0.11	-21.4 ± 1.3	0.517 ± 0.056
	Pooled	**4.24 ± 0.09**	**-15.9 ± 1.0**	**0.464 ± 0.043**
Daytime	2007	2.84 ± 0.09	-5.74 ± 1.11	0.404 ± 0.046
	2008	2.00 ± 0.08	-7.27 ± 0.94	0.201 ± 0.039
	2009	1.99 ± 0.07	-3.21 ± 0.90	0.0998 ± 0.0374
	2010	1.90 ± 0.10	-10.7 ± 1.2	0.283 ± 0.052
	Pooled	**2.14 ± 0.09**	**-7.00 ± 1.06**	**0.267 ± 0.044**
Nighttime	2007	2.73 ± 0.08	-11.0 ± 0.9	0.303 ± 0.039
	2008	2.05 ± 0.07	-13.4 ± 0.8	0.225 ± 0.034
	2009	1.28 ± 0.08	-8.29 ± 0.94	0.101 ± 0.038
	2010	1.59 ± 0.10	-15.7 ± 1.2	0.255 ± 0.049
	Pooled	**2.05 ± 0.09**	**-14.0 ± 1.0**	**0.216 ± 0.042**
All-day	**Observed**	**3.72 ± 2.35**	**-0.29 ± 1.57**	**$0.54 +\!/\!- 0.73$**

3.3. MLR analysis of observational data

We used MLR to test for significant relationships between meteorological drivers and AF in the observed data from 1995 to 2011. The results were non-significant for all meteorological drivers ($p > 0.1$; $n = 17$) and moderate correlations were detected amongst the observed meteorological variables, especially air temperature and relative humidity ($r = -0.63$) (Crawford and Duchon, 1999; Table 4). However, the observational data revealed the same effect direction on AF for each of the meteorological driver variables, and similar effect magnitudes for air temperature and RH (Table 3). The coefficient estimates for air temperature and RH were within 16% of the estimates derived using pooled, all-day simulation data, but wind speed showed greater differences. However, due to the non-significance of the observed coefficients, this was not investigated further.

3.4. Suitability of linear models

The MLR models were able to reproduce the GLM-AED-simulated AF reasonably well, except for scenarios resulting in substantial decreases in the simulated AF. With all three meteorological driver predictors included in a statistical model, they together explained 60, 25, and 26% of the variation in the AF in the all-day, daytime, and nighttime scenarios, respectively. Analysis of the residual plots for the all-day MLR model showed linearity, nor-

mality, and homoscedasticity, suggesting that the ΔAF response can be adequately represented by a linear combination of ΔAT, ΔWS and ΔRH (residual plots not shown). Correlations amongst the simulated meteorological drivers were all non-significant, which was an outcome of the random perturbation design (Table 4). Additionally, the AF values calculated from pooled MLR models showed linear agreement with GLM-AED-simulated AF (Fig. 8), further suggesting that the linear model is adequate (i.e. comparable with GLM-AED) to capture the effects of the meteorological variables on the AF. However, in cases where GLM-AED predicted large decreases in AF, there were deviations from linearity because the MLR models predicted less extreme decreases in AF (Fig. 8a & b). This usually occurred in cases of a negative ΔAT, positive ΔWS and negative ΔRH (i.e. all meteorological driver perturbations acting to decrease AF).

3.5. Application of linear models

The effect of perturbations in the meteorological drivers cannot be compared directly because of differences in units. However, the climate projections discussed in Section 2.6. Climate scenarios can be coupled with the MLR results to calculate the approximate potential impact of each meteorological driver on AF. An air temperature increase of 3 °C would lead to an approximate increase of 12.7 days season^{-1} in AF; a wind speed decrease of -0.25 m s^{-1} corresponds to an increase in AF of 4.0 days season^{-1}; an RH increase of
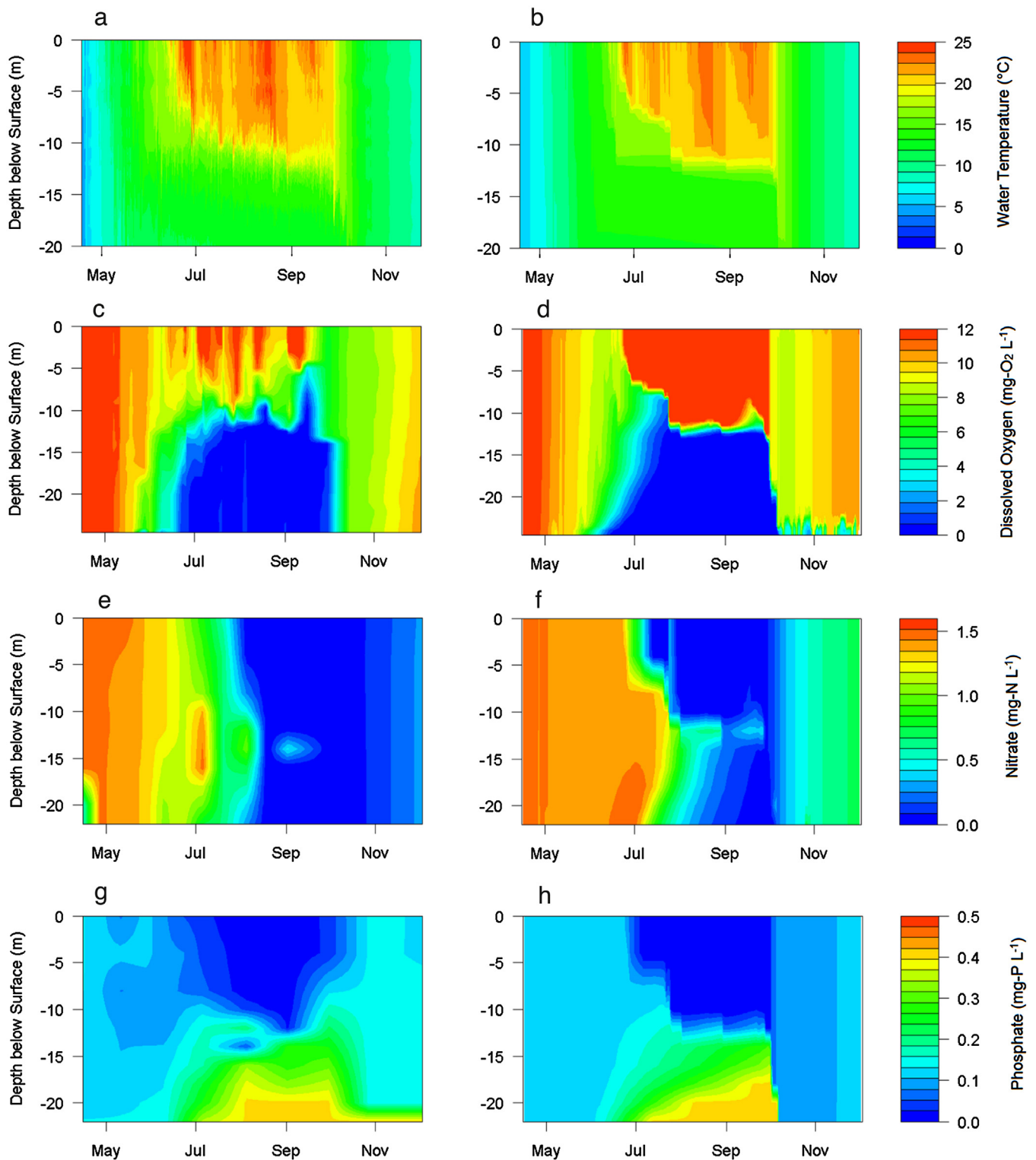
Fig. 4. Visual comparison of observed (left panels) and simulated (right panels) data for select state variables for the 2009 open water season: (a and b) water temperature; (c and d) dissolved oxygen; (e and f) nitrate; (g and h) phosphate.

Table 4
Meteorological driver variable correlation coefficients with p-value in parentheses for observed (lower/left section) and scenario (upper/right section) data.

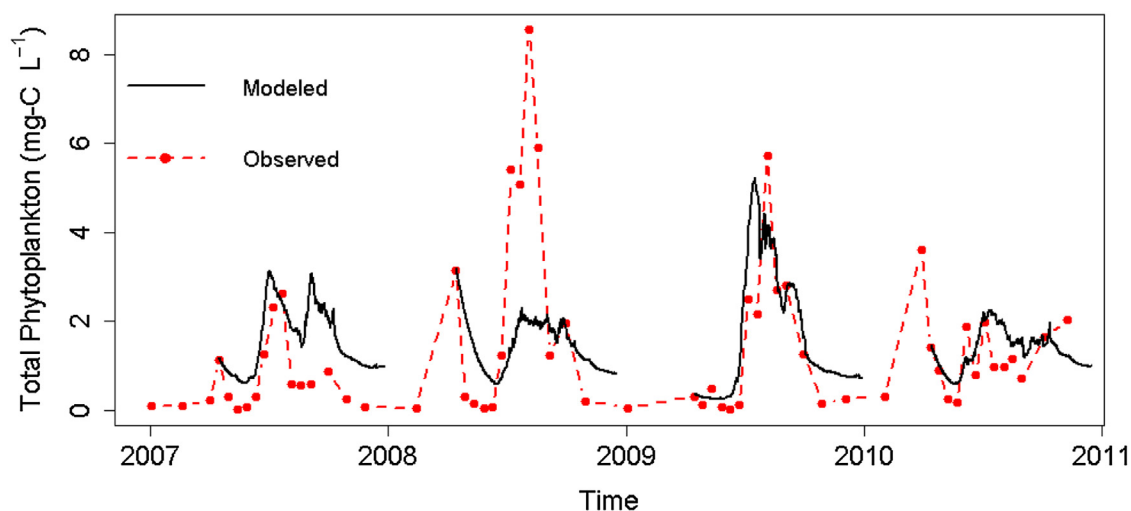| Observed\Modeled	Air Temp.	Wind Speed	Relative Humidity
Air Temp.	1	−0.031 (0.15)	0.0018 (0.93)
Wind Speed	0.382 (0.13)	1	0.0007 (0.97)
Relative Humidity	−0.63 (0.007)	−0.33 (0.20)	1

Fig. 5. Comparison of observed and simulated mean total phytoplankton concentration (0–8 m depth) for the simulated period of 2007–2010.
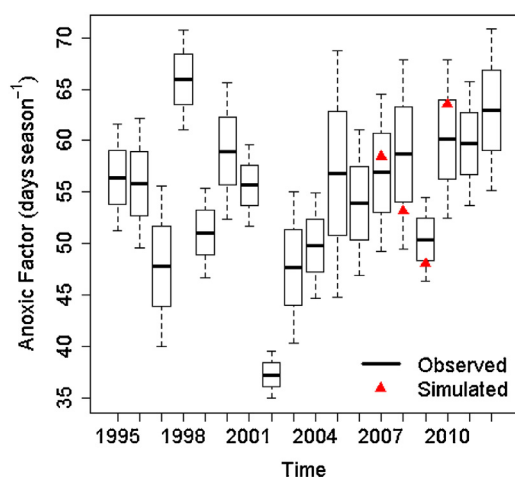

Fig. 6. Time series of observed anoxic factor derived from NTL-LTER oxygen measurements for the period 1995–2012, with simulated values shown for 2007–2010. Whiskers show the minimum and maximum possible anoxic factor values given the temporal gaps in the observed oxygen data. Black bars represent the mean of the extremes, and the boxes represent the lower and upper quartiles.

6% corresponds to an increase in AF of 2.8 days season^{-1}. Therefore, of the three meteorological drivers we investigated, air temperature has by far the greatest potential for impact on AF during the latter half of the 21st century, followed by wind speed and then RH.

3.6. Extremes testing results

The simulated AF exhibited a range of approximately 0–120 days season^{-1} across the state space represented by meteorological driver perturbations of air temperature $\pm15\,^{\circ}$C, wind speed $\pm2\,\mathrm{m\,s^{-1}}$, and RH ±15% (Fig. 9). It is clear from the response surfaces that there are many states (all points along any contour line) that result in the same AF. For example, an increase in air temperature accompanied by an increase in wind speed could yield the same AF as the baseline scenario. The highest simulated AF values resulted from simultaneous increases in air temperature and decreases in wind speed. The most extreme scenarios included in this analysis, while not expected to occur as a result of changing climate, led to AF values as high as 120 days season^{-1}, which is more than twice the normal AF value for Lake Mendota. The lowest simulated AF value was 0 days season^{-1} (no anoxia), most notably

occurring under scenarios of decreased air temperature (greater than 5 $^{\circ}$C decrease) and increased wind speed (greater than 1 m s^{-1} increase). While again an unlikely scenario to be observed in the future for Lake Mendota, this underscores the powerful influence that meteorological drivers have on the oxic environment in a lake ecosystem.

4. Discussion

4.1. Application of linear models

We interpreted the relative importance of a given meteorological driver variable based on the range of simulated AF values across the climate change scenarios. As discussed in Section 3.5. *Application of linear models,* air temperature has by far the greatest potential for impact on AF, followed by wind speed and then RH. However, increases in AF, driven by predicted increases in air temperature (Katt-Reinders and Pomplun, 2011) may be dampened by changes in other meteorological variables that have the opposite effect on AF. For example, increased wind speed could lead to later stratification onset, earlier stratification breakdown, and decreased thermal stability during stratified periods, all resulting in decreased AF. These offsetting effects are clear in our air temperature/wind speed response surface (Fig. 9a), and demonstrated elsewhere (Kerimoglu and Rinke, 2013).

Across all of our scenario simulations, the range of AF predicted from GLM-AED was ±15 days season^{-1} (black boxes in Fig. 9), and was within the range of the observed system (Fig. 6). This natural inter-annual variability could intensify climate driven increases in AF. Higher AF may enhance regeneration of phosphorus and promote greater phytoplankton blooms (Lopez-Urrutia, 2008; Wagner and Adrian, 2009) and potentially lead to summertime fish kills for species requiring the colder temperatures of the hypolimnion (Fang et al., 2004).

The diurnal asymmetry of the meteorological variable effects on AF suggest that it is important to drive numerical simulation models with sub-daily meteorological data. We observed that the daily mean value of a meteorological variable may not capture the full effect of that driver on the lake system. For example, Lake Zurich epilimnetic temperatures have been increasing at about the same rate as daily minimum air temperatures, which is at a faster rate than the daily mean air temperature (Livingstone, 2003). If simulations are run without sub-daily data, responses like this could be completely suppressed. Therefore, models could potentially under-
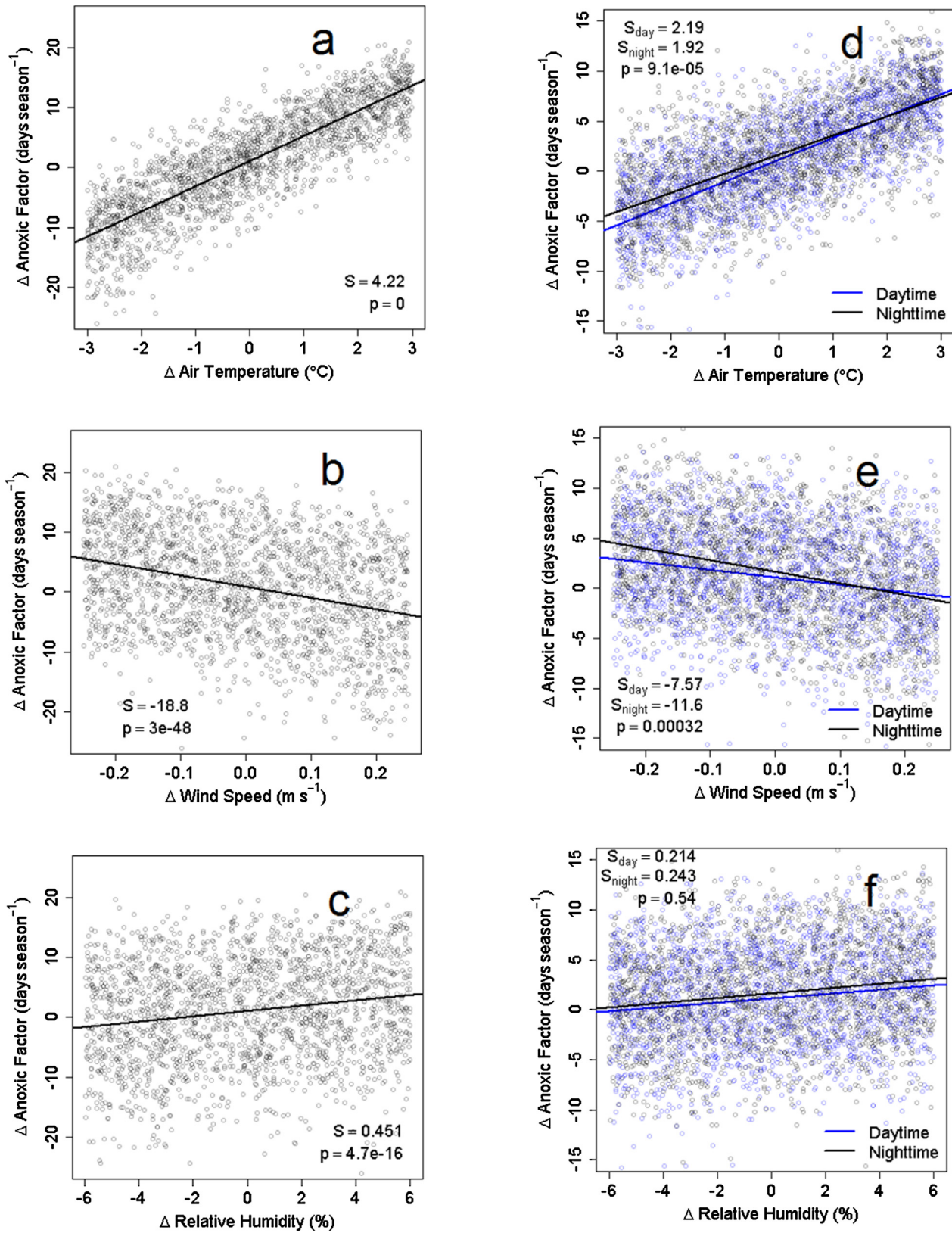
Fig. 7. Comparison of effects (slope) of meteorological driver variables on anoxic factor for all-day, daytime and nighttime exposure to perturbations. Each point is a scenario simulation. In each plot, the anoxic factor was regressed on a given meteorological driver variable, with underlying random perturbations in the remaining two meteorological driver variables. Panels a, b, and c show the simple linear regression lines for air temperature, wind speed, and relative humidity, respectively (S = slope, p = p-value for nonzero effect). In panels d, e, and f, S_{day} = daytime slope/effect; S_{night} = nighttime slope/effect; p = p-value for statistically significant difference in slope between day and night.
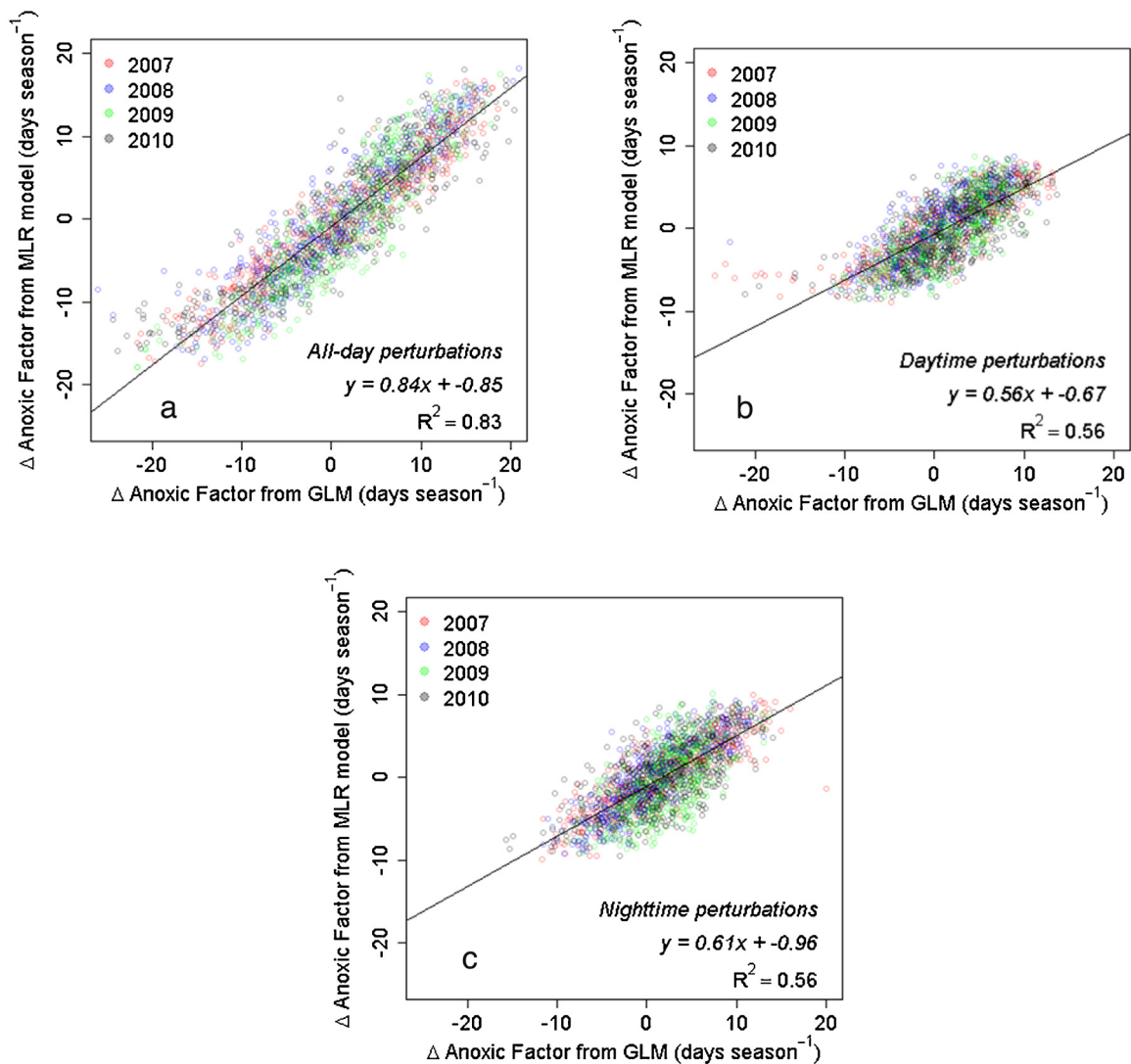
Fig. 8. Regression comparison of results from the MLR models and the GLM-AED simulations for the (a) all-day model, (b) daytime model, and (c) nighttime model.

estimate future changes in lake ecosystems, especially for those regions projected to experience diurnal asymmetry in the meteorological variables themselves.

4.2. MLR analysis of simulation results

Diurnal asymmetry in driving variables may be an important factor in determining how lakes respond to future changes in meteorology. AF may be more sensitive to nighttime changes in wind speed as the lake becomes more responsive to wind mixing. Equivalent daytime changes would be dampened by the stratifying forces imposed by surface heating. Our results showing the greater importance of daytime air temperature to AF (Fig. 7d) are in contrast to studies of two European lakes that conclude that the daily minimum air temperature (occurring generally during the night) is important for controlling epilimnetic temperature and thermal stability (Livingstone 2003; Wilhelm et al., 2006). The discrepancy with the two previously mentioned studies may result from the fact that Lake Müggelsee was analyzed only during the stratified period (Wilhelm et al., 2006), and Lake Zurich does not experience complete turnover each year (Livingstone, 2003). In contrast, Lake Mendota is reliably dimictic, and our analyses extended beyond the stratified period to include turnover in the spring and fall. It is possible that nighttime air temperature tends to have a stronger

influence on lake thermal structure and AF during stratified periods, and daytime air temperature has greater importance during isothermal periods. If this is the case, the strong daytime air temperature influence during isothermal periods may have outweighed the nighttime air temperature influence during stratified periods in our study, resulting in a stronger net influence of daytime air temperature influence on AF through the entire open water period. Simulations focused on mixing regimes might help resolve this issue. Finally, we did not see a statistical difference between the effects of daytime and nighttime RH perturbations on AF. Although RH has been found to be significant in determining the equilibrium temperature of the lake epilimnion (Wilhelm et al., 2006), there was no significant difference between day and night effects on AF within the range of projected changes in mean monthly RH ($\pm 6\%$).

In Lake Mendota, anoxia duration accounted for a much larger portion of the simulated AF variability than did mean thermocline depth (78% and 21%, respectively), likely because of the sensitivity of lake thermal structure to destratifying forces, especially around the transition periods between homothermy and stratification. For example, a single windy day in the autumn when the lake is cooling and at a low level of thermal stability could induce turnover and complete mixing. However, this same windy day during the mid-summer when the lake is strongly stratified might only deepen the thermocline slightly. Under these circumstances,
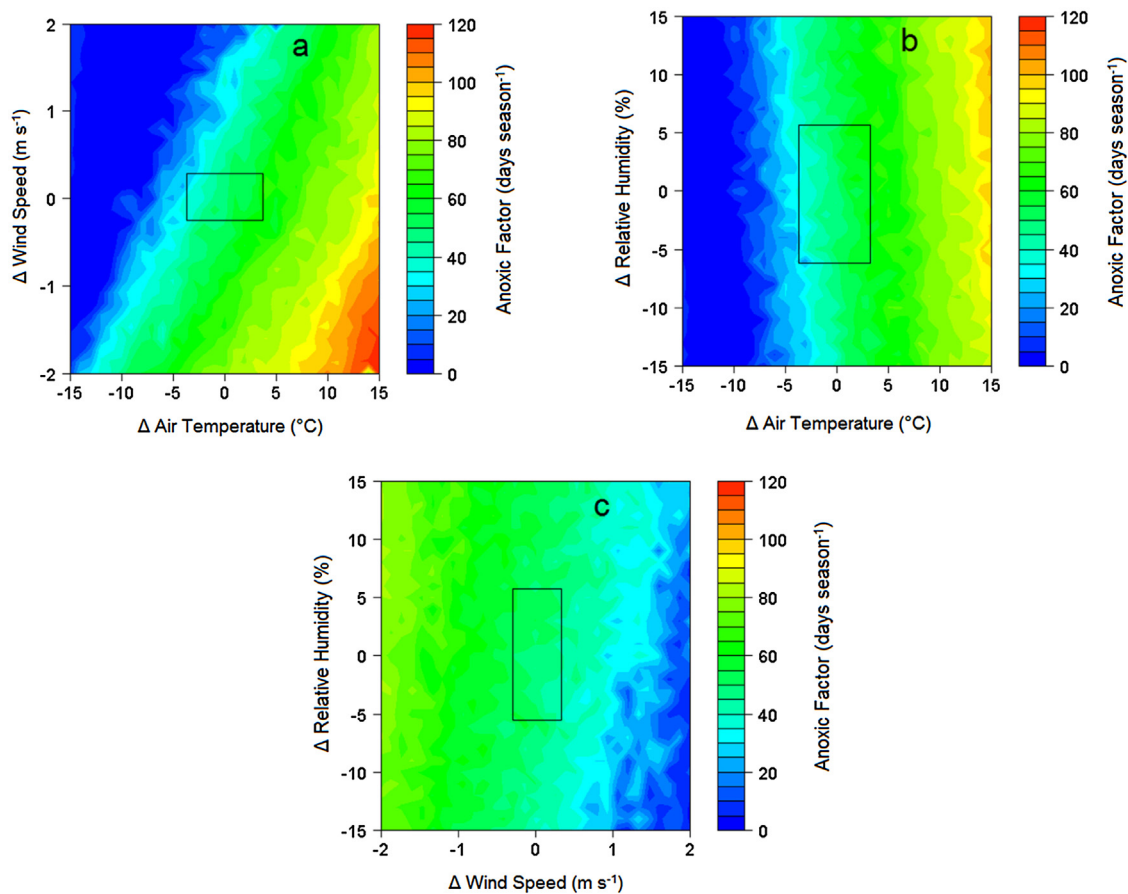
Fig. 9. Response surface plots for the response of the GLM-AED-simulated anoxic factor to simultaneous perturbations in two meteorological driver variables: (a) air temperature/wind speed, (b) air temperature/relative humidity, and (c) wind speed/relative humidity. Black rectangles approximate the state space included in the meteorological scenarios used the regression analyses.

the windy autumn day has the potential to reduce AF by days or even weeks compared to the baseline, whereas the windy summer day would likely reduce the AF (by reducing anoxia area) by just fractions of equivalent anoxia days. This relationship is influenced by lake morphometry, as a perfectly cylindrical lake with a flat bottom would not be influenced by mean thermocline depth since the anoxic sediment area would be constant regardless of the anoxic depth. Finally, our finding that stratification onset and decay accounted for approximately equal variability of anoxia duration across the scenarios is likely an artifact of our scenarios using constant meteorological driver perturbations across the entire open water season. Further investigations that apply time-variable perturbations should yield more insight on how timing and intensity of aberrations in meteorological drivers will affect AF and other emergent properties.

Our analysis of the relationships between the meteorological drivers and physical, chemical and biological lake state indices showed strong relationships between the meteorological drivers and lake physics, and weaker relationships between the meteorological drivers and lake chemistry and biology. Due to physical-biological coupling, any perturbation to a driver will affect all physical, chemical and biological state variables to some degree, often in ways that are difficult to interpret. However, our results show that strong relationships exist between meteorological drivers, lake thermal structure, and hypolimnetic anoxia, and that the projected rise in mean air temperatures will likely lead to increased spatial and temporal extent of anoxia in temperate, eutrophic lakes.

4.3. Suitability of linear models

Simple linear models may not adequately predict ecosystem responses to extreme meteorological forcing or to subtle differences in diurnal variability. The MLR models accounted for 83% of the variability in the simulated AF for the all-day perturbations and 56% of the variability in the simulated AF for both the daytime and nighttime perturbations (Fig. 7). The MLR models performed worse for the daytime and nighttime perturbation scenarios likely because of increased nonlinear effects when the meteorological driver perturbations are applied for only part of the day, instead of consistently across all hours of the day. Still, this is good agreement considering a reduction in the number of model parameters of two orders of magnitude from GLM-AED to the 3-parameter statistical model. However, in each case (all-day, daytime and nighttime) the least-squares line through the points has a slope of <1 (Fig. 7), meaning that the MLR models tended to predict less extreme changes in AF as compared to GLM-AED. This is again likely due to nonlinear processes that are captured by GLM-AED but not by the simple data-based MLR model. Therefore, the MLR models are able to provide a ΔAF estimate that is generally in agreement with GLM-AED, but the MLR models become less reliable as the magnitude of the meteorological driver perturbations increase and the nonlinear process effects become more apparent. This is especially evident in the 'tails' extending from the data point clusters in Fig. 7a-b where the points fall well above the least squares line, indicating that the MLR model under-predicted the decrease in AF. Interestingly, these tail points were generated under scenarios in which perturbations in air temperature, wind speed, and relative humidity all acted

to decrease AF, but not when the meteorological drivers acted to increase AF. This suggests that GLM-AED processes that strengthen stratification (and tend to increase AF) are more linear than GLM-AED processes that weaken stratification (and tend to decrease AF). Since stratification breakdown occurs in the model when the available mixing energy exceeds the resistance to mixing due to density stratification (Hipsey et al., 2014), the high nonlinearity observed in the stratification breakdown process may be the result of these thresholds being exceeded.

4.4. Goodness-of-fit

The fit between simulated and observed data as measured by NMAE was within literature ranges for all commonly reported state variables, except for epilimnetic DO, DOC and DIC (Table 2). For DO, hypolimnetic DO was very well simulated (NMAE ≈ 0.16), and the NMAE for whole-lake DO was only slightly higher (worse) than the literature range. The simulations overestimated epilimnetic DO, most likely as a result of exclusion of zooplankton from the model, leading to overestimated primary production. We evaluated whether the overestimation of epilimnetic DO had an effect on our overall conclusions by artificially increasing phytoplankton respiration parameters (leading to decreased DO) such that the NMAE for all depths was approximately 0.20. The increase in phytoplankton respiration reduced the goodness-of-fit for most other state variables, especially phytoplankton. However, the results derived from these simulations yielded the same conclusions as did the original simulations: all instances of significant ($p < 0.01$) effects of meteorological drivers, and significant differences in effects between altering meteorological drivers during only daytime and nighttime, remained the same. Additionally, the MLR coefficients (effects) remained within ~10% of the original results. These findings suggest that the simulated epilimnetic DO is satisfactory and that our inferences about the anoxic factor are not particularly sensitive to modest changes in phytoplankton net primary production. The fits for DOC and DIC were worse than values reported by Kara et al., 2012. However the shorter simulation period (~90 days) and lack of major changes in thermal structure (i.e. no mixing events) in Kara et al. (2012)'s study likely resulted in a better fit for their data. The fit metrics for DOC and DIC were satisfactory in comparison to most other commonly-reported chemical state variables; all NMAE values were ≤0.34, compared to an average chemical state variable NMAE value of 0.51 reported in Kara et al. (2012). Finally, despite known challenges of biological calibration (Rigosi et al., 2011), our model sufficiently captured total phytoplankton dynamics, with the notable exception of a large *Aphanizomenon* bloom (Fig. 5), highlighting the critical need for further progress in simulation of phytoplankton blooms.

4.5. Conclusion & looking forward

Our study focused on the effects of changes in surface energy forcing on anoxia. We found that the projected rise in mean air temperatures will likely lead to increased spatial and temporal extent of anoxia in temperate, eutrophic lakes. Changes in water balance and nutrient loading could have significant effects on anoxia as well, potentially through alterations in mixing and oxygen demand. Future numerical simulation studies should seek to investigate anoxia response, as well as other chemical and biological responses, to changes in exogenous drivers across a gradient of lake types- including differences in morphometry, mixing regimes, climatic exposure, water transparency, and trophic states. Future studies should also seek to build on progress in numerical simulation of phytoplankton, especially extreme events, as phytoplankton drive critical physical and chemical feedbacks through water transparency and nutrient distribution, and have important aesthetic and health consequences for lakes and reservoirs. Finally, as computing, data collection, and modeling resources continue to advance, the integration of climate, watershed, and lake models has the potential to provide a deeper understanding of interactions between climate, land use and water resources in our rapidly changing and increasingly complex environment.

Appendix A.

Table A1
Default values and final assigned values for calibrated GLM parameters. Default values in the table are the default values from the 'coldlake' example simulation available on the GLM website. All parameters not included in this table retained default values as presented in the GLM science manual.

Parameter Name	Description	Units	Default Value	Assigned Value
min_layer_thick	Minimum layer thickness	m	0.5	0.1
max_layer_thick	Maximum layer thickness	m	1.5	1.0
K_w	Extinction coefficient for PAR radiation	m^{-1}	0.2	0.25
ch	Bulk aerodynamic coefficient for sensible heat transfer	–	0.0013	0.00132
ce	Bulk aerodynamic coefficient for latent heat transfer	–	0.0013	0.00112
coef_wind_drag	Bulk aerodynamic coefficient for transfer of momentum	–	0.0013	0.00121
coef_mix_conv	Mixing efficiency − convective overturn	–	0.2	0.272
coef_wind_stir	Mixing efficiency − wind stirring	–	0.23	0.278
coef_mix_shear	Mixing efficiency − shear production	–	0.3	0.286
coef_mix_turb	Mixing efficiency − unsteady turbulence (acceleration)	–	0.51	0.526
coef_mix_KH	Mixing efficiency − Kelvin- Helmholtz turbulent billows	–	0.3	0.341
coef_mix_hyp	Mixing efficiency of hypolimnetic turbulence	–	0.5	0.453

Table A2
Default values and final assigned values for calibrated AED parameters. Defaults are the parameter values from the AED science manual or Kara et al. (2012) providing the best initial fit. All parameters not included in this table retained default values as presented in the AED science manual.

Parameter Name	Description	Units	Default Value	Assigned Value
theta_sed_oxy	Temperature multiplier for temperature dependence of sediment oxygen flux	–	1.08	1.065
Ksed_oxy	Half saturation constant for oxygen dependence of sediment oxygen flux	mmol O_2/m^3	46.875	51.57
Fsed_oxy	Maximum flux of oxygen across the sediment water interface into the sediment	mmol O_2/m^2/d	−14.375	−12.55
theta_sed_frp	Temperature multiplier for temperature dependence of sediment phosphate flux	–	1.08	1.032
Ksed_frp	Half saturation constant for oxygen dependence of sediment phosphate flux	mmol O_2/m^3	62.5	69.54
Fsed_frp	Maximum flux of oxygen across the sediment water interface into the sediment	mmol P/m^2/d	0.4036	0.591
theta_sed_nit	Temperature multiplier for temperature dependence of sediment nitrate flux	–	1.08	1.055
Ksed_nit	Half saturation constant for oxygen dependence of sediment nitrate flux	mmol O_2/m^3	1562.5	1563
Fsed_nit	Maximum flux of nitrate across the sediment water interface into the sediment	mmol N/m^2/d	−8.5	−9.466
Rdenit	Maximum rate of denitrification	1/d	0.05	0.065
Kdenit	Half saturation constant for oxygen dependence of denitrification	mmol O_2/m^3	12.5	15.24
theta_sed_doc	Temperature multiplier for temperature dependence of sediment DOC flux	–	1.08	1.085
theta_doc_miner	Temperature multiplier for temperature dependence of DOC mineralization rate	–	1.08	1.09
Ksed_doc	Half saturation constant for oxygen dependence of sediment DOC flux	mmol O_2/m^3	15.626	16.81
Rdoc_miner	Maximum rate of mineralization of DOC	1/d	0.01	0.015
Fsed_doc	Maximum flux of DOC across the sediment water interface into the sediment	mmol C/m^2/d	0.01	0.0440
theta_sed_dic	Temperature multiplier for temperature dependence of sediment DIC flux	–	1.08	1.021
Ksed_dic	Half saturation constant for oxygen dependence of sediment DIC flux	mmol O_2/m^3	20	24.338
Fsed_dic	Maximum flux of DIC across the sediment water interface into the sediment	mmol C/m^2/d	3	4.908
theta_sed_amm	Temperature multiplier for temperature dependence of sediment ammonium flux	–	1.08	1.139
Ksed_amm	Half saturation constant for oxygen dependence of sediment ammonium flux	mmol O_2/m^3	62.5	65.747
Fsed_amm	Maximum flux of ammonium across the sediment water interface into the sediment	mmol N/m^2/d	22.127	22.158
theta_sed_rsi	Temperature multiplier for temperature dependence of sediment silica flux	–	1.08	1.030
Ksed_rsi	Half saturation constant for oxygen dependence of sediment silica flux	mmol O_2/m^3	150	153.51
Fsed_rsi	Maximum flux of silica across the sediment water interface into the sediment	mmol Si/m^2/d	1.8 (0.6 in science manual)	0.975

Table A3
Default values and final assigned values for calibrated AED phytoplankton parameters. Default values are not presented as they do not necessarily reflect the biological characteristics of the phytoplankton functional groups modeled in this study. All parameters not included in this table retained default values as presented in the AED science manual.

Parameter Name	Description	Units	Microcystis	Aphanizomenon	Chlorophytes	Diatoms
Pmax	Maximum phytoplankton growth rate of 20 °C	1/d	1.9	2.1	2.1	1.0
Tstd	Standard temperature	°C	19	24	20	19
Topt	Optimum temperature	°C	24	27	23	14
Tmax	Maximum temperature	°C	35	35	33	21
vT	Arrhenius temp scaling coefficient for growth	–	1.089	1.101	1.099	1.109
kr	Phytoplankton respiration/metabolic loss rate of 20 °C	1/d	0.0748	0.0900	0.0545	0.0642
vr	Arrhenius temperature scaling for phytoplankton respiration	–	1.075	1.140	1.033	1.057

References

Arend, K.K., Beletsky, D., DePinto, J.V., Ludsin, S.A., Roberts, J.J., Rucinski, D.K., Scavia, D., Schwab, D.J., Höök, T.O., 2011. Seasonal and interannual effects of hypoxia on fish habitat quality in central Lake Erie. Freshw. Biol. 56, 366–383.

Arhonditsis, G.B., Adams-Vanharn, B.A., Nielsen, L., Stow, C.A., Reckhow, K.H., 2006. Evaluation of the current state of mechanistic aquatic biogeochemical modeling: citation analysis and future perspectives. Environ. Sci. Technol. 40, 6547–6554.

Bouffard, D., Ackerman, J.D., Boegman, L., 2013. Factors affecting the development and dynamics of hypoxia in a large shallow stratified lake: hourly to seasonal patterns. Water Resour. Res. 49, 2380–2394.

Brock, T.D., 1985. A Eutrophic Lake: Lake Mendota, Wisconsin. Springer, New York.

Bruce, L.C., Hamilton, D., Imberger, J., Gal, G., Gophen, M., Zohary, T., Hambright, K.D., 2006. A numerical simulation of the role of zooplankton in C, N and P cycling in Lake Kinneret, Israel. Ecol. Modell. 193, 412–436.

Carpenter, S.R., Stanley, E.H., Vander Zanden, M.J., 2011. State of the world's freshwater ecosystems: physical, chemical, and biological changes. Annu. Rev. Environ. Resour. 36, 75–99.

Cooke, G.D., Welch, E.B., Peterson, S., Nichols, S.A., 2005. Restoration and Management of Lakes and Reservoirs. CRC Press.

Crawford, T.M., Duchon, C.E., 1999. An improved parameterization for estimating effect atmospheric emissivity for use in calculating daytime downwelling longwave radiation. J. Appl. Meteorol. 38, 474–480.

Diaz, R.J., 2001. Overview of hypoxia around the world. J. Environ. Qual. 30, 275–281.

Fang, X., Stefan, H.G., Eaton, J.G., McCormick, J.H., Alam, S.R., 2004. Simulation of thermal/dissolved oxygen habitat for fishes in lakes under different climate scenarios Part 1. Cool-water fish in the contiguous US. Ecol. Modell. 172, 13–37.

Foley, B., Jones, I.D., Maberly, S.C., Rippey, B., 2012. Long-term changes in oxygen depletion in a small temperate lake: effects of climate change and eutrophication. Freshw. Biol. 57, 278–289.

Gal, G., Hipsey, M.R., Parparov, A., Wagner, U., Makler, V., Zohary, T., 2009. Implementation of ecological modeling as an effective management and investigation tool: lake Kinneret as a case study. Ecol. Modell. 220, 1697–1718.

Hamilton, D.P., Schladow, S.G., 1997. Prediction of water quality in lakes and reservoirs. Part I – model description. Ecol. Modell. 96, 91–110.

Hampton, S.E., Izmest'Eva, L.R., Moore, M.V., Katz, S.L., Dennis, B., Silow, E.A., 2008. Sixty years of environmental change in the world's largest freshwater lake – Lake Baikal, Siberia. Global Change Biol. 14, 1947–1958.

Hanson, P.C., Pollard, A.I., Bade, D.L., Predick, K., Carpentar, S.R., Foley, J.A., 2004. A model of carbon evasion and sedimentation in temperate lakes. Global Change Biol. 10, 1285–1298.

Hipsey, M.R., Bruce, L.C., Hamilton, D.P., 2013. Aquatic Ecodynamic (AED) Model Library- Science Manual.

Hipsey, M.R., Bruce, L.C., Hamilton, D.P., 2014. General Lake Model (GLM)- Model Overview and User Information (v1.4.0).

Hostetler, S.W., Alder, J.R., Allan, A.M., 2011. Dynamically Downscaled Climate Simu- Lations over North America: Methods, Evaluation and Supporting Documentation for Users. U.S. Geological Survey Reston, Virginia, OFR 2011-1238, pp. 64.

Jeppesen, E., Meerhoff, M., Jacobsen, B.A., Hansen, R.S., Søndergaard, M., Jensen, J.P., Lauridsen, T.L., Mazzeo, N., Branco, C.W.C., 2007. Restoration of shallow lakes by nutrient control and biomanipulation—the successful strategy varies with lake size and climate. Hydrobiologia 581, 269–285.

Jeppesen, E., Kronvang, B., Meerhoff, M., Søndergaard, M., Hansen, K.M., Andersen, H.E., Lauridsen, T.L., Liboriussen, L., Beklioglu, M., Ozen, A., Olesen, J.E., 2009. Climate change effects on runoff, catchment phosphorus loading and lake ecological state, and potential adaptations. J. Environ. Qual. 38, 1930–1941.

Kamarainen, A.M., Yuan, H.L., Wu, C.H., Carpenter, S.R., 2009. Estimates of phosphorus entrainment in Lake Mendota: a comparison of one-dimensional and three- dimensional approaches. Limnol. Oceanogr. 7, 553e567.

Kara, E.L., Hanson, P., Hamilton, D., Hipsey, M.R., McMahon, K.D., Read, J.S., Winslow, L., Dedrick, J., Rose, K., Carey, C.C., Bertilsson, S., da Motta Marques, D., Beversdorf, L., Miller, T., Wu, C., Hsieh, Y.-F., Gaiser, E., Kratz, T., 2012. Time-scale dependence in numerical simulations: assessment of physical,

chemical, and biological predictions in a stratified lake at temporal scales of hours to months. Environ. Modell. Softw. 35, 104–121.

Katt-Reinders, E., Pomplun, S., 2011. Wisconsin's changing climate: impacts and adaptation. In: Wisconsin Initiative on Climate Change Impacts.

Kerimoglu, O., Rinke, K., 2013. Stratification dynamics in a shallow reservoir under different hydro-meteorological scenarios and operational strategies. Water Resour. Res. 49, 7518–7527.

Kitchell, J.F., 1992. Food Web Management: a Case Study of Lake Mendota. Springer-Verlag, New York.

Livingstone, D.M., 2003. Impact of secular climate change on the thermal structure of a large temperate Central European Lake. Clim. Change 57, 205–225.

Lopez-Urrutia, A., 2008. The metabolic theory of ecology and algal bloom formation. Limnol. Oceanogr. 53, 2046–2047.

Müller, B., Bryant, L.D., Matzinger, A., Wüest, A., 2012. Hypolimnetic oxygen depletion in eutrophic lakes. Environ. Sci. Technol. 46, 9964–9971.

Mackay, M.D., Neale, P.J., Arp, C.D., De Senerpont Domis, L.N., Fang, X., Gal, G., Jöhnk, K.D., Kirillin, G., Lenters, J.D., Litchman, E., Macintyre, S., Marsh, P., Melack, J., Mooij, W.M., Peeters, F., Quesada, A., Schladow, S.G., Schmid, M., Spence, C., Stokes, S.L., 2009. Modeling lakes and reservoirs in the climate system. Limnol. Oceanogr. 54, 2315–2329.

Marcé, R., Rodríguez-Arias, M.À., García, J.C., Armengol, J., 2010. El Niño Southern Oscillation and climate trends impact reservoir water quality. Global Change Biol. 16, 2857–2865.

Nürnberg, G.K., 1988. A simple method for predicting the date of fall turnover in thermally stratified lakes. Limnol. Oceanogr. 33, 1190–1195.

Nürnberg, G.K., 1995. Quantifying anoxia in lakes. Limnol. Oceanogr. 40, 1100–1111.

Nelder, J.A., Mead, R., 1965. A simplex method for function minimization. Comput. J. 7, 308–313.

North, R.P., North, R.L., Livingstone, D.M., Köster, O., Kipfer, R., 2014. Long-term changes in hypoxia and soluble reactive phosphorus in the hypolimnion of a large temperate lake: consequences of a climate regime shift. Global Change Biol. 20, 811–823.

Palmer, M.E., Yan, N.D., Somers, K.M., 2014. Climate change drives coherent trends in physics and oxygen content in North American lakes. Clim. Change 124, 285–299.

R Development Core Team, 2014. R: A Language and Environment for Statistical Computing. R Foundation for Statistical Computing.

Read, J.S., Winslow, L.A., Hansen, G.J.A., Van Den Hoek, J., Hanson, P.C., Bruce, L.C., Markfort, C.D., 2014. Simulating 2368 temperate lakes reveals weak coherence in stratification phenology. Ecol. Modell. 291, 142–150.

Rigosi, A., Marcé, R., Escot, C., Rueda, F.J., 2011. A calibration strategy for dynamic succession models including several phytoplankton groups. Environ. Modell. Softw. 26, 697–710.

Robertson, D.M., Imberger, J., 1994. Lake number, a quantitative indicator of mixing used to estimate changes in dissolved oxygen. Int. Rev. Hydrobiol. 79, 159–176.

Samal, N.R., Pierson, D.C., Schneiderman, E., Huang, Y., Read, J.S., Anandhi, A., Owens, E.M., 2012. Impact of climate change on Cannonsville Reservoir thermal structure in the New York City water supply. Water Qual. Res. J. Can. 47, 389–405.

Schneider, P., Hook, S.J., 2010. Space observations of inland water bodies show rapid surface warming since 1985. Geophys. Res. Lett. 37, L22405.

Trolle, D., Skovgaard, H., Jeppesen, E., 2008. The water framework directive: setting the phosphorus loading target for a deep lake in Denmark using the 1D lake ecosystem model DYRESM–CAEDYM. Ecol. Modell. 219, 138–152.

Trolle, D., Hamilton, D.P., Pilditch, C.A., Duggan, I.C., Jeppesen, E., 2011. Predicting the effects of climate change on trophic status of three morphologically varying lakes: implications for lake restoration and management. Environ. Modell. Softw. 26, 354–370.

Wagner, C., Adrian, R., 2009. Cyanobacteria dominance: quantifying the effects of climate change. Limnol. Oceanogr. 54, 2460–2468.

Wilhelm, S., Hintze, T., Livingstone, D.M., Adrian, R., 2006. Long-term response of daily epilimnetic temperature extrema to climate forcing. Can. J. Fish. Aquat. Sci. 63, 2467–2477.

Williamson, C.E., Saros, J.E., Vincent, W.F., Smol, J.P., 2009. Lakes and reservoirs as sentinels, integrators, and regulators of climate change. Limnol. Oceanogr. 54, 2273–2282.